Hydrologic connectivity between landscapes and streams: Transferring reach- and plot-scale understanding to the catchment scale

Kelsey G. Jencso,[1] Brian L. McGlynn,[1] Michael N. Gooseff,[2] Steven M. Wondzell,[3] Kenneth E. Bencala,[4] and Lucy A. Marshall[1]

[1] The relationship between catchment structure and runoff characteristics is poorly understood. In steep headwater catchments with shallow soils the accumulation of hillslope area (upslope accumulated area (UAA)) is a hypothesized first-order control on the distribution of soil water and groundwater. Hillslope-riparian water table connectivity represents the linkage between the dominant catchment landscape elements (hillslopes and riparian zones) and the channel network. Hydrologic connectivity between hillslope-riparian-stream (HRS) landscape elements is heterogeneous in space and often temporally transient. We sought to test the relationship between UAA and the existence and longevity of HRS shallow groundwater connectivity. We quantified water table connectivity based on 84 recording wells distributed across 24 HRS transects within the Tenderfoot Creek Experimental Forest (U.S. Forest Service), northern Rocky Mountains, Montana. Correlations were observed between the longevity of HRS water table connectivity and the size of each transect's UAA ($r^2 = 0.91$). We applied this relationship to the entire stream network to quantify landscape-scale connectivity through time and ascertain its relationship to catchment-scale runoff dynamics. We found that the shape of the estimated annual landscape connectivity duration curve was highly related to the catchment flow duration curve ($r^2 = 0.95$). This research suggests internal catchment landscape structure (topography and topology) as a first-order control on runoff source area and whole catchment response characteristics.

Citation: Jencso, K. G., B. L. McGlynn, M. N. Gooseff, S. M. Wondzell, K. E. Bencala, and L. A. Marshall (2009), Hydrologic connectivity between landscapes and streams: Transferring reach- and plot-scale understanding to the catchment scale, *Water Resour. Res.*, *45*, W04428, doi:10.1029/2008WR007225.

1. Introduction

[2] Transferring plot and reach-scale hydrologic understanding to the catchment scale and elucidating the link between catchment structure and runoff response remains a challenge. En route to addressing this dilemma many recent advances in catchment hydrology have focused on the discretization, function, and connection of catchment landscape elements according to their topographic [*Welsch et al.*, 2001; *Seibert and McGlynn*, 2007], hydrologic [*McGlynn et al.*, 2004], and hydrochemical [*Covino and McGlynn*, 2007] attributes. In steep mountain catchments with relatively uniform soil depths and organized drainages, dominant landscape elements can often be reduced to hillslope, riparian, and stream zones. Hydrologic connections between hillslope-riparian-stream (HRS) zones occur when water table continuity develops across their interfaces and streamflow is present.

[3] Development of water table connectivity between riparian and hillslope zones has been associated with threshold behavior in catchment-scale runoff production [*Devito et al.*, 1996; *Sidle et al.*, 2000; *Buttle et al.*, 2004], mechanisms of rapid delivery of pre-event water [*McGlynn et al.*, 2002; *McGlynn and McDonnell*, 2003b], dissolved carbon dynamics [*McGlynn and McDonnell*, 2003a] and nutrient transport [*Creed et al.*, 1996; *Vidon and Hill*, 2004], at various timescales. Identifying the spatial and temporal hydrologic connectivity of runoff source areas within a catchment is an important step in understanding how landscape level hydrologic dynamics lead to whole catchment hydrologic and solute response.

[4] In forested mountain landscapes hillslopes comprise the major landscape element. Hillslope soils are often shallow and located on moderate to steep slopes. Hillslopes typically have relatively low antecedent wetness due to their steep slopes and well drained soils. During periods of high wetness hillslope soils can be highly transmissive and contribute significant quantities of water to near stream areas and the stream network [*Peters et al.*, 1995; *McGlynn and McDonnell*, 2003b]. This hydrologic connectivity is

[1]Department of Land Resources and Environmental Sciences, Montana State University, Bozeman, Montana, USA.

[2]Department of Civil and Environmental Engineering, Pennsylvania State University, University Park, Pennsylvania, USA.

[3]Olympia Forestry Sciences Laboratory, Pacific Northwest Research Station, U.S. Forest Service, Olympia, Washington, USA.

[4]U.S. Geological Survey, Menlo Park, California, USA.

requisite for the flushing of solutes and nutrients downslope through the riparian zone to the stream [*Creed et al.*, 1996; *Buttle et al.*, 2001; *Stieglitz et al.*, 2003].

[5] Riparian zones (near stream areas) are located between the hillslope and stream interfaces, in topographic lows, often at the base of organized hillslope drainages and can remain at or near saturation with minor to modest water table fluctuations in the upper soil profile. Characteristics of riparian zones often include anoxic conditions, high organic matter content, and low hydraulic conductivity associated with the predominance of organic, silt and clay sized particles. These characteristics lead to potential buffering of hillslope inputs of water [*McGlynn et al.*, 1999; *McGlynn and Seibert*, 2003] and nutrients [*Burt et al.*, 1999; *Hill*, 2000; *Carlyle and Hill*, 2001; *McGlynn and McDonnell*, 2003a] to streams.

[6] At the plot scale, it has been shown that hillslope and riparian elements can exhibit independent water table dynamics, characteristic of each landscape element [*Seibert et al.*, 2003; *Ocampo et al.*, 2006]. These investigations demonstrated that the steady state assumption of uniform groundwater rise and fall across the landscape is often unrealistic. Timing differences between hillslope and riparian water table dynamics were attributed to different antecedent soil moisture deficits and drainage characteristics.

[7] Research at the catchment scale has also cited water table connectivity between riparian and hillslope landscape elements as a first-order control on solute and runoff response. *McGlynn et al.* [2004] related riparian water table dynamics, hillslope runoff contributions, and total runoff in five nested catchments to landscape topography and the organization of hillslope and riparian landscape elements. Increasing synchronicity of runoff and solute response across scales was attributed to increasing antecedent wetness, event size, and the resulting increased riparian-hillslope landscape hydrologic connectivity.

[8] These previous studies highlight the importance of HRS connectivity for the explanation and prediction of hydrologic response. However, they lacked either spatial or temporal coverage, thus providing little insight into spatiotemporal upland to stream connectivity and its controlling variables. A framework combining high-frequency, spatially distributed, source area connectivity observations along with a metric of their important hydrogeomorphic attributes is needed to link internal source area response to runoff dynamics as measured at the catchment outlet.

[9] In steep mountain catchments topographic convergence and divergence and the accumulation of contributing area are considered important hydrogeomorphic controls on the conductance of subsurface water from hillslopes to riparian and stream zones [*Freeze*, 1972]. Many of the formative hillslope hydrology studies [*Hewlett and Hibbert*, 1967; *Dunne and Black*, 1970; *Harr*, 1977; *Anderson and Burt*, 1978; *Beven*, 1978] observed increased subsurface water accumulation in areas with topographically convergent hillslopes and higher upslope accumulated area (UAA). Upslope accumulated area is the area of land draining to a particular point in the landscape and has also been referred to as local contributing area. While topographically convergent areas often exhibit higher UAA, the same UAA magnitude is possible with a range of upslope morphologies or shapes (degrees of convergence and divergence).

[10] We sought to investigate the hydrogeomorphic controls on HRS hydrologic connectivity, their spatial and temporal distributions, and their implications for catchment-scale runoff generation. We combined digital elevation model (DEM) based terrain analyses with high-frequency water table measurements across 24 HRS transitions at catchment scales ranging from 0.4 to 17.2 km^2 to address the following questions: (1) Does the size of hillslope UAA explain the development and persistence of HRS water table connectivity? (2) Can topographic analysis be implemented to scale observed transect HRS hydrologic connections to the stream network and catchment scales? (3) How do spatial patterns and frequency of landscape hydrologic connectivity relate to catchment runoff dynamics? We present a framework for quantifying the spatial distribution of runoff source areas and exploring the spatially explicit links between source area connectivity and runoff generation.

2. Site Description

[11] This study was conducted in the Tenderfoot Creek Experimental Forest (TCEF) (lat. 46.55′N, long. 110.52′W), located in the Little Belt Mountains of the Lewis and Clark National Forest in Central Montana (Figure 1). The research area consists of seven gauged catchments that form the headwaters of Tenderfoot Creek (22.8 km^2), which drains into the Smith River, a tributary of the Missouri River.

[12] The climate of the Little Belt Mountains is continental with occasional Pacific maritime influence along the Continental Divide. Annual precipitation averages 840 mm. Monthly precipitation generally peaks in December or January (100 to 120 mm per month) and declines to a late July through October dry period (45 to 55 mm per month). Approximately 75% of the annual precipitation falls during November through May, predominantly as snow. During the study period (1 October 2006 to 1 October 2007), 845 mm of precipitation was recorded; 688 mm as snow and 157 mm as rain. Peak runoff typically occurs in late May or early June and is generated by snowmelt or rain on snow events. Lowest flows occur from August through the winter months.

[13] Upland areas of the experimental forest are dominated by lodgepole pine. Sedges (*Carex* spp.) and rushes (*Juncaceae* spp.) dominate riparian vegetation in headwater areas with fine silt and clay textured soils and where water tables are generally near the surface. Willows (*Salix* spp.) dominate riparian areas where water tables are deeper and soils are coarsely textured.

[14] The seven TCEF gauged subcatchment areas range in size from 3 to 22.8 km^2. Catchment headwater zones are typified by moderately sloping (average slope $\sim$8°) extensive (up to 1200 m long) hillslopes and variable width riparian zones. Treeless parks are prominent at the headwaters of each catchment. Approaching the main stem of Tenderfoot Creek the streams become more incised, hillslopes become shorter (<500 m) and steeper (average slope $\sim$20°), and riparian areas narrow relative to the catchment headwaters.

[15] Major soil groups in the TCEF are loamy Typic Cryochrepts located along hillslope positions and clayey Aquic Cryoboralfs in riparian zones and parks [*Holdorf*, 1981]. Riparian soils are 0.5−2.0 m deep, dark colored clay loams and gravelly loams high in organic matter.
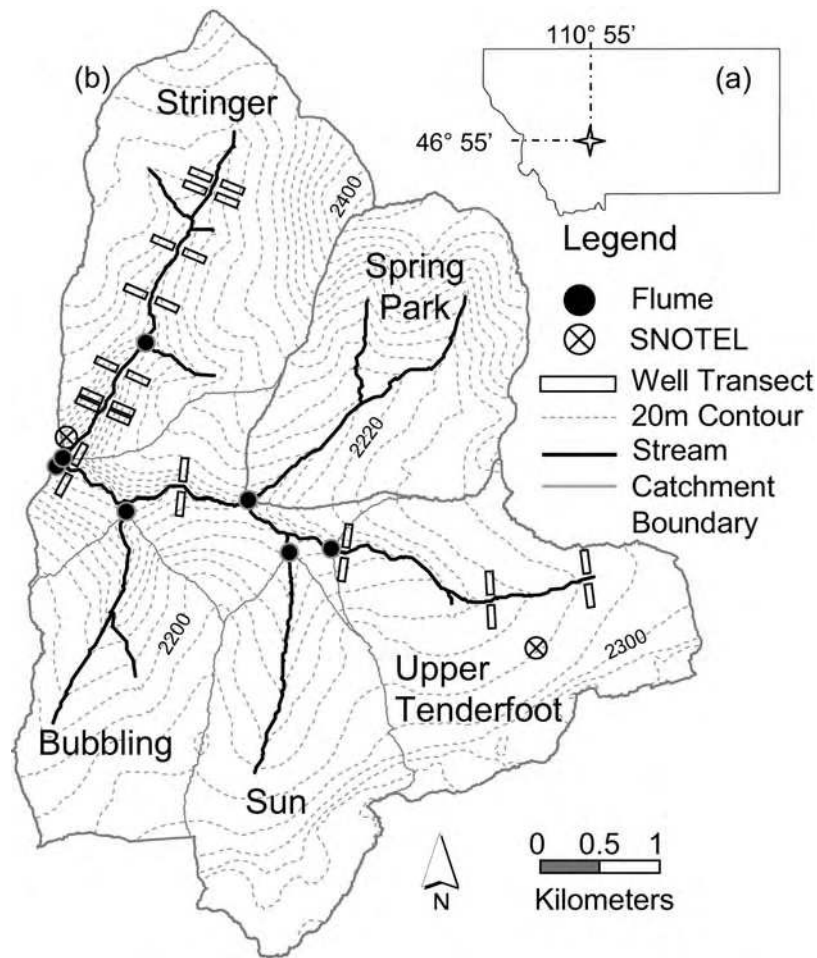
Figure 1. Site location and instrumentation of the Tenderfoot Creek Experimental Forest (TCEF) catchment. (a) Catchment location in the Rocky Mountains, Montana. (b) Catchment flumes, well transects, and SNOTEL instrumentation locations. Transect extents are not drawn to scale.

[16] The parent material consists of igneous intrusive sills of quartz porphyry, Wolsey shales, Flathead quartzite and granite gneiss[*Farnes et al.*, 1995]. Basement rocks of granite gneiss occur at lower elevations and are frequently seen as exposed, steep cliffs and talus slopes depending on landscape position. Flathead sandstone overlies the gneiss in mid catchment positions, followed by Wolsey shale and gentler slopes in headwater areas.

[17] Historic records dating from 1996 to the present are available for climatologic and hydrologic variables, courtesy of United States Forest Service (USFS) instrumentation. Two snow survey telemetry (SNOTEL) stations located in TCEF (Onion Park, 2259 m, and Stringer Creek, 1996 m) record real-time data on snow depth, snow water equivalent, precipitation, radiation, and wind speed. Hydrologic monitoring of the Experimental Forest includes seven flumes and one weir for eight gauged catchments where continuous streamflow is measured with stream level recorders (Figure 1).

[18] TCEF is an ideal site for the development of new techniques for linking landscape characteristics to water table and runoff response because it includes numerous catchments with a full range of upslope extents and degrees of topographic divergence and convergence. Topography is characterized by few sinks (i.e., digital elevation model

(DEM) grid cell with no neighboring cells with lower elevations than itself) and a clear distinction between hillslope and riparian landscape elements. Soil depths are relatively consistent across hillslope (0.5–1.0 m) and riparian (1–2.0 m) zones with localized upland areas of deeper soils. In addition, the abundance of existing infrastructure and historic data provide a wealth of information regarding past hydrologic response to climatic variables.

3. Methods

3.1. Landscape Analysis

[19] We selected 24 hillslope-riparian-stream transects based on preliminary terrain analysis of a coarse 30 m USGS DEM, later refined with 1 m resolution airborne laser swath mapping (ALSM) data (courtesy of the National Center for Airborne Laser Mapping-NCALM). Upstream contributing areas at each transect (watershed areas) ranged from 0.41 to 17.2 km^2, each composed of a range of hillslope and riparian UAA, as well as slope, aspect, and other terrain variables. We installed control points along Stringer and Tenderfoot Creek and at all flume locations with a Trimble survey grade GPS 5700 receiver operating in "fast static mode". All GPS control points were accurate to
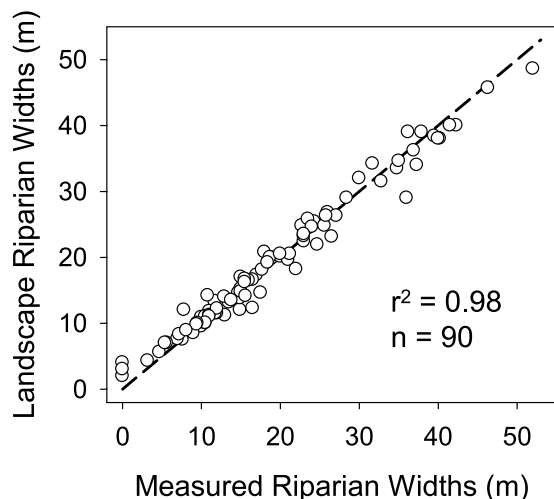
Figure 2. Measured versus terrain analysis derived riparian widths. The dashed line is the 1:1 line. The slope of the regression was 0.93, and the *y* intercept was 1.4 m.

within 1–5 cm. From these control points we performed surveys of Stringer and Tenderfoot Creek thalwegs, flume locations at each subcatchment outlet, well locations along each transect, and riparian zone extents. Survey data was corroborated with the ALSM derived DEM.

[20] The TCEF stream network, riparian areas, hillslope areas, and terrain indices were delineated using ALSM DEMs at 1, 3, 5, 10, and 30 m grid cell resolutions. ALSM elevation measurements were achieved at a horizontal sampling interval of the order <1 m, with vertical accuracies of ±0.05 to ±0.15 m. ALSM data provided a detailed, 1 × 1 m grid cell DEM.

[21] Quantification of each transect's hillslope and riparian UAA followed landscape analysis methods developed by *Seibert and McGlynn* [2007]. The first step in this landscape analysis approach was to compute the stream network from the DEM using a creek threshold area method corroborated with field reconnaissance. Depending on the time of year (spring snowmelt versus summer base flow) many of the stream heads in TCEF shift in location along the channel. The creek threshold initiation area was estimated as 40 ha based on field surveys of channel initiation points in TCEF. Channel initiation points were identified with morphological indicators (scoured streambeds, defined banks, and incisions into the ground surface) set forth by *Dietrich and Dunne* [1993].

[22] UAA for each stream cell, or the lateral area flowing into the stream network, was calculated using a triangular multiple flow-direction algorithm (MD∞) [*Seibert and McGlynn*, 2007]. Once the accumulated area exceeded the 40 ha threshold value, it was routed downslope as "creek area" and all cells along the downslope flow path were labeled "creek cells". The UAA measurements for each transect's hillslope were taken at the toe-slope (transition from hillslope to riparian zone) well position. Additional coverages generated from the base DEM were local inflows of UAA to each stream cell separated into contributions from each side of the stream (T. Grabs et al., manuscript in preparation, 2009), the topographic index [*Beven and Kirkby*, 1979], and catchment area at each stream cell.

[23] The TCEF riparian areas were mapped using a DEM analysis threshold method, whereby all accumulated area less than two meters in elevation above the stream cell it flows into was designated as riparian area. To compare the 2 m threshold landscape analysis derived riparian widths to actual riparian widths at TCEF, we surveyed 90 riparian cross sections in Stringer Creek, Spring Park Creek, and Tenderfoot Creek. Riparian-hillslope boundaries were determined in the field based on breaks in slope, soil characteristics (i.e., gleying, organic accumulation, color, and texture), and terrain characteristics. A regression relationship ($r^2 = 0.97$) corroborated our terrain based riparian mapping (Figure 2).

3.2. Hydrometric Monitoring

[24] We recorded liquid precipitation at 15 min intervals with tipping bucket rain gauges (Texas Electronics 525MM-L, 0.1 mm increments). Rain gauges were installed at ST1, ST4, and a riparian eddy-covariance tower near ST2. Additional hourly precipitation measurements were obtained from gauges at National Resources Conservation Service SNOTEL stations located near the Lower Stringer flume (1996 m) and near (2259 m) the headwaters of Tenderfoot Creek. SNOTEL measurements were also used for hourly measurements of snow depth and snow water equivalent. Runoff was measured for each of seven gauged catchments using three H-flumes and four Parshall flumes. Stage at each flume was recorded at 30 min intervals with float potentiometers (USFS) and TruTrack, Inc., water level capacitance rods (±1 mm resolution).

3.3. Hillslope-Riparian Shallow Water Table Measurements

[25] We monitored 24 transect locations, located along 12 stream network positions, spanning a range of hillslope and riparian slope and UAA combinations (landscape element assemblages). Individual transects reflect the respective difference in UAA inputs and riparian widths on either side of the stream. UAA inflows and riparian extents on each side of the stream were independent of one another due to differential convergence and divergence of catchment topography and hillslope lengths (T. Grabs et al., manuscript in preparation, 2009). Fourteen transects were installed along Stringer Creek (Figure 1) and ten were installed along Tenderfoot Creek (Figure 1). Transects along Stringer Creek are referred to as ST1 through 7, followed by an E (east) or W (west) and those along Tenderfoot Creek are referred to as TFT1 through 5, followed by an N (north) or S (south). In all cases, transects are numbered sequentially, with 1 designating the most upstream transect.

[26] Transects consisted of three to six wells (84 total) located on the lower hillslope (1–5 m above the break in slope), toe-slope (the break in slope from riparian to hillslope zones), and riparian zone (1 m from stream channel), along groundwater flow paths to the stream. Additional riparian wells were installed 5–10 m upstream of the riparian and toeslope wells to ascertain the direction of groundwater flow and shifts in direction during events using 3-point triangulation of total potential gradients. Wells consisted of 1.5 inch diameter PVC conduit screened across the completion depth to 10 cm below the ground surface. Completion depths to bedrock ranged from 0.8 to 1.5 m on hillslopes to 1–2.0 m in the riparian zones. These comple-
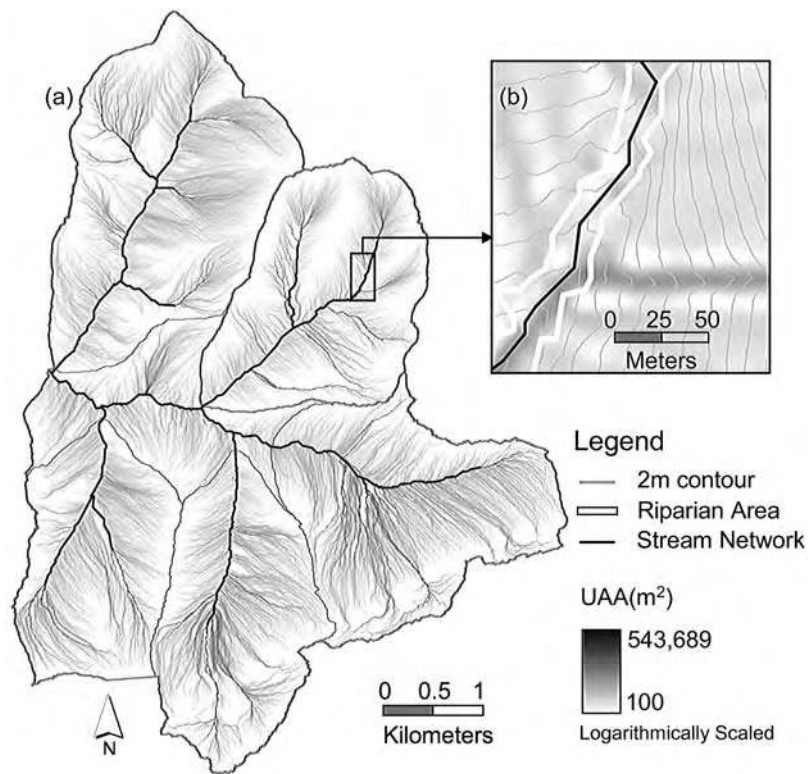
Figure 3. TCEF. (a) Upslope accumulated area (UAA) for each pixel and (b) an example riparian area extent derived from terrain analysis.

tion depths are corroborated by ~12 soil pits excavated to bedrock and 100s of soil probe depth measurements across hillslope to riparian transitions. Wells were installed with a solid steel rod inserted into the PVC casing. The rod and well casing were driven until refusal at the bed rock boundary and the rod removed. A clay seal and small mound derived from local materials was applied to prevent surface water intrusion. Well water levels were recorded at 30 min intervals with TruTrack, Inc., capacitance rods. Complementary water level measurements were collected weekly using an electric water level tape to corroborate capacitance rod measures.

[27] Hydrologic connectivity between HRS zones was inferred from the presence of saturation measured in well transects spanning the hillslope, toeslope, and riparian positions. We define a hillslope-riparian-stream connection as a time interval during which streamflow occurred and both the riparian and adjacent hillslope wells recorded water levels above bedrock. We do not discern between the mechanisms responsible for water table development and HRS water table connectivity, rather if, when, and for how long water table connectivity was present.

4. Results

4.1. Landscape Analysis

[28] We resampled the original 1 m DEM to determine the DEM cell size that was most robust for relating water table dynamics and UAA. The 1 m ALSM derived DEM was sampled discretely to obtain 3, 5, 10 and 30 m cell size DEMs. When implementing the flow accumulation/UAA algorithms, the 3 m and 5 m DEMs appeared more

susceptible to micro topographic influences such as fallen trees, boulders, etc., which exert negligible control on subsurface water redistribution. Conversely, the 30 m grid size was too coarse to reflect slope breaks between riparian and hillslope transitions and observed convergence and divergence in upland areas. The 10 m DEM provided a realistic representation of the topography, reflecting convergence and divergence and providing the most robust relation to water table dynamics observed across all 24 well transects (Figure 3). Tables 1 and 2 summarize subcatchment area, hillslope UAA (measured at each transects toe-slope well location), riparian widths, and the slope and soil depths of hillslope and riparian zones for transects located in the Stringer and Tenderfoot Creek catchments, respectively.

4.2. Snowmelt and Precipitation Characterization

[29] We present snow accumulation and melt data from the Upper Tenderfoot Creek (relatively flat 0° aspect, elevation 2259 m) SNOTEL site (Figure 4). Rainfall data are presented from the Stringer Transect 1 rain gauge (elevation 2169 m). During the base flow observation period (1 October 2006 to 27 April 2007), snow fall increased the snowpack snow water equivalent (SWE) to a maximum of 358 mm. Twenty-two minor melt events, ranging from 5 to 10 mm, occurred during this base flow period. Springtime warming lead to an isothermal snowpack and most of the snowpack melted between 27 April 2007 and 19 May 2007. Average daily SWE losses were 15 mm and reached a maximum of 35 mm on 13 May 2007. A final spring snow fall and subsequent melt occurred between 24 May 2007 and 1 June 2007, yielding 97 mm of water. Four days following the end of snowmelt, the rain period was

Table 1. Tenderfoot Creek Transect Characteristics

Transect	Catchment Area (km^2)	UAA (m^2)	Riparian Width (m)	Hillslope (deg slope)	Riparian (deg slope)	Hillslope Soil Depth (m)	Riparian Soil Depth (m)	HRS Connectivity (% of year)
TFT1N	0.42	8,151	8	5.5	3.3	1.0–1.10	1.20–1.50	27
TFT1S	0.42	11,152	12	3.6	2.8	1.0–1.10	0.80–1.0	22
TFT2N	1.37	5,044	3.8	4.8	2.3	0.90–1.20	0.95–1.0	24
TFT2S	1.37	32,111	19.6	5.8	1.8	0.75–2.50	1.0–1.45	61
TFT3N	4.33	2,367	8.5	17.7	2.2	0.60–0.85	0.60–1.20	0
TFT3S	4.33	7,070	7.2	23	9.5	0.90–1.0	0.70–1.20	15
TFT4N	13.16	25,753	9.3	22	7.7	0.20–0.55	0.70–0.85	40
TFT4S	13.16	1,186	4.4	42	2.9	0.60–1.0	0.50–0.75	0
TFT5N	17.21	1,527	9.1	26	5.2	0.60–0.75	0.70–0.85	4
TFT5S	17.21	7,842	2.9	37	6.8	0.20–0.50	0.55–0.75	7

initiated with a series of low-intensity rain storms (4–7 June 2007 and 13–18 June 2007), totaling 30 and 22 mm respectively. Following this rain period the recessional period began. Precipitation inputs during the recession period were minor, except for one summer thunderstorm on 26 July 2007 yielding 34 mm of rain over a 7 h period. Total precipitation inputs (snowmelt and rain) to the TCEF catchment over the course of the 2007 water year totaled 845 mm.

4.3. Detailed Description of HRS Water Table Response Dynamics

[30] Detailed results for a subset of transects characteristic of the primary HRS landscape assemblages found within TCEF, their associated water table responses, and their hydrologic connectivity frequency and duration are presented in Appendix A and illustrated in Figure 5.

4.4. Summary of HRS Water Table Dynamics and Connections According to UAA

[31] The 24 transects of HRS assemblages demonstrated clear differences in groundwater connectivity as a function of their UAA size (Figure 6). While this relationship is continuous, we describe three general UAA typologies to emphasize the degree to which the range of transects exhibited a hydrologic connection. Transects with small

UAA (699–3869 m^2) generally exhibited no HRS connection or a rapid and transient connection during large events (Figures 5i, 5k, 5p, 6x, and Figure 6a). When the time of their connectivity was summed for the 2007 water year these transects were connected no longer than 14% of the water year. Excluding ST2E which exhibited a 14% connection with only 3000 m^2 UAA, the small sized UAA transects remained connected for only up to 4% of the water year, primarily during peak snowmelt and rain event periods.

[32] Transects with UAA size ranging from 4900–32,100 m^2 generally exhibited a more sustained hydrologic connectivity during large snowmelt and rain events (Figures 5a, 5f, 5n, 5s, and Figure 6b). Transient connectivity was observed for these midranged areas during base flow or recession periods in response to isolated snowmelt or rain events. Annual connectivity ranged from 3 to 61% of the water year, primarily during the snowmelt and recession periods when larger UAA transects reflected persistent water tables from drainage of their extensive upslope areas.

[33] Two transects, ST2W and ST5W, were installed with UAA sizes of 44,395 and 46,112 m^2, respectively. These transects exhibited continuous HRS connectivity (Figure 5u and Figure 6c). Though HRS connections were not measured for areas with UAA above 46,000 m^2, there are TCEF catchment locations with larger sized UAA. Visual obser-

Table 2. Stringer Creek Transect Characteristics

Transect	Catchment Area (km^2)	UAA (m^2)	Riparian Width (m)	Hillslope (deg slope)	Riparian (deg slope)	Hillslope Soil Depth (m)	Riparian Soil Depth (m)	HRS Connectivity (% of year)
ST1W	1.26	1,563	12.7	12.5	4.2	0.80–0.95	0.60–1.0	0
ST1E	1.26	10,165	11.8	15.6	5.9	0.60–1.30	0.60–1.05	8
ST2W	1.39	44,395	21	8.6	6	0.70–1.20	0.70–2.0	100
ST2E	1.39	3,000	8.3	18.15	6.2	0.95–1.30	1.0–1.50	14
ST3W	2.98	3,869	11.7	19.6	2.9	1.0–1.35	0.50–1.0	2
ST3E	2.98	3,029	6.5	19.8	2	0.80–1.40	1.0–1.30	2
ST4W	3.59	699	4.7	22	7.5	0.80–1.0	0.95–1.0	0
ST4E	3.59	4,930	9.9	21	8	0.60–1.40	1.0–1.15	19
ST5W	4.80	46,112	16.5	20.8	5.07	0.90–1.0	0.70–1.80	100
ST5E	4.80	1,923	7.7	26	7	0.90–1.40	1.0–1.50	3
ST6W	5.17	6,176	9.7	21	6.9	0.80–1.0	1.10–1.35	7
ST6E	5.17	3,287	4.5	36	10.3	1.0–1.50	0.65–1.0	0
ST7W	5.27	6,201	9	27	7.5	0.90–1.10	0.80–1.10	3
ST7E	5.27	9,854	8.8	28	7.4	0.90–1.0	1.10–1.40	10
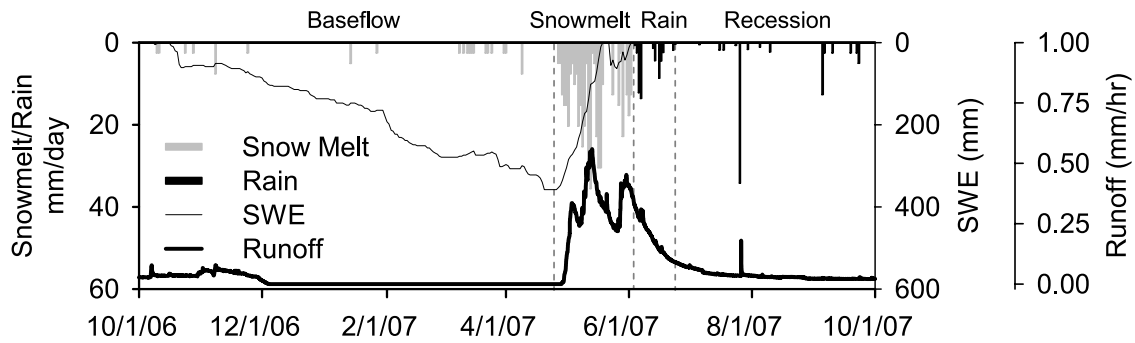
Figure 4. Snow and rainwater inputs, snow water equivalent (SWE), and runoff separated into base flow, snowmelt, rain, and recession observation periods.

vations along these extensive, highly convergent hillslopes and headwater areas, confirmed the presence of near surface water tables above the break in slope as well as surface saturated conditions year-round in their associated riparian zones.

[34] The timing of the connection and disconnection of HRS zones also varied according to UAA. Transects with midrange UAA lagged the transient hillslope responses of low UAA transects during early snowmelt, but were more sustained once a hillslope water table was established (Figures 6a and 6b).

4.5. Scaling Source Area Connectivity to an Entire Stream Network

[35] Patterns across transects indicated a strong UAA influence on the timing and persistence of connectivity between streams and their associated riparian and hillslope zones. To further explore the UAA-connectivity duration relationship we regressed the total time each HRS transect was connected during the 2007 water year against the size of UAA at their hillslope to riparian transition. The duration of HRS water table connectivity was highly correlated ($r^2 = 0.91$) to the size of each transects UAA (Figure 7; equation (1)):

$$\%TimeConnected = (0.00002*UAA - 0.0216)*100. \quad (1)$$

We also tested the topographic index [Beven and Kirkby, 1979] but did not find improved explanatory power ($r^2 = 0.84$).

[36] We applied equation (1) to all of the UAA inflows along the entire Tenderfoot Creek stream network to assess catchment-scale connectivity distributions and elucidate their implications for catchment-scale hydrologic response. Lateral inflows of UAA for each stream cell were separated into their component left and right side UAAs using an algorithm developed by T. Grabs et al. (manuscript in preparation, 2009). HRS water table connectivity was heterogeneous from reach to reach along Tenderfoot Creek according to the location of UAA inputs (Figure 8). The majority (70%) of the stream network comprises small UAAs in the size range of 0 to 5000 m^2 (Figure 9a). HRS connectivity for these areas was estimated between 0 to 8% of the year. Medium ranged UAA reaches (5,000–30,000 m^2) composed ~25% (Figure 9a) of the network and were estimated connected between 8 and 62% of the year. The remaining 5% of the stream network included

large headwater areas and convergent hillslope hollows with UAA in the size range of 30,000 to ~75,000 m^2 (Figure 9a). These UAA sizes were estimated to be connected for 62 to 100% of the year.

[37] We compared Tenderfoot Creek's connectivity duration curve (CDC) to the catchment annual flow duration curve (FDC) to assess how HRS connectivity was related to catchment level hydrologic response (Figures 9b and 10a and 10b). The FDC was derived from 8762 hourly observations of runoff at the Lower Tenderfoot flume for the 2007 water year. The CDC was derived from the combined 10 m left and right stream bank frequencies (3108 10 m cells) of HRS connectivity for the 2007 water year (equation (1)).

[38] The CDC and FDC for Tenderfoot Creek were highly correlated (Figures 9b and 10a), suggesting a relationship between the amount of the stream network connected to its uplands and streamflow magnitude. While the annual regression was strong ($r^2 = 0.95$ Figure 10a), we also investigated the regression relationships for each of three flow states (base flow, transition, and wet) and found differential predictive power in each period (Figure 10b). Approximately 55% of the year during the driest periods (fall and winter base flow) the lowest runoff values 0.015–0.03 mm/h were associated with the lowest amount (<4%) of HRS connectivity across the stream network. During the transition from dry to wet times (~35% of the year) more HRS assemblages became connected and runoff increased to 0.10 mm/h. Divergence between the CDC and FDC was greatest during this transitional period. The FDC showed a sharp increase at 0.06 mm/h runoff while the CDC increased gradually. Peak snowmelt and large rain events (~10% of the time) resulted in the highest network connectivity (up to 67%) which was associated with peak runoff up to a maximum of 0.54 mm/h and close correspondence between the FDC and CDC.

5. Discussion

[39] Streams, riparian zones, and hillslopes have been intensively studied at small spatial scales (stream reaches < 1 km, plots of 10–100 m^2). At the other end of the spectrum, entire catchments have been studied without explicit understanding of how their internal landscape hydrologic processes are distributed, interact, or integrate across the stream network to produce whole watershed behavior. This has resulted in detailed plot and reach-specific process understanding with little transferability
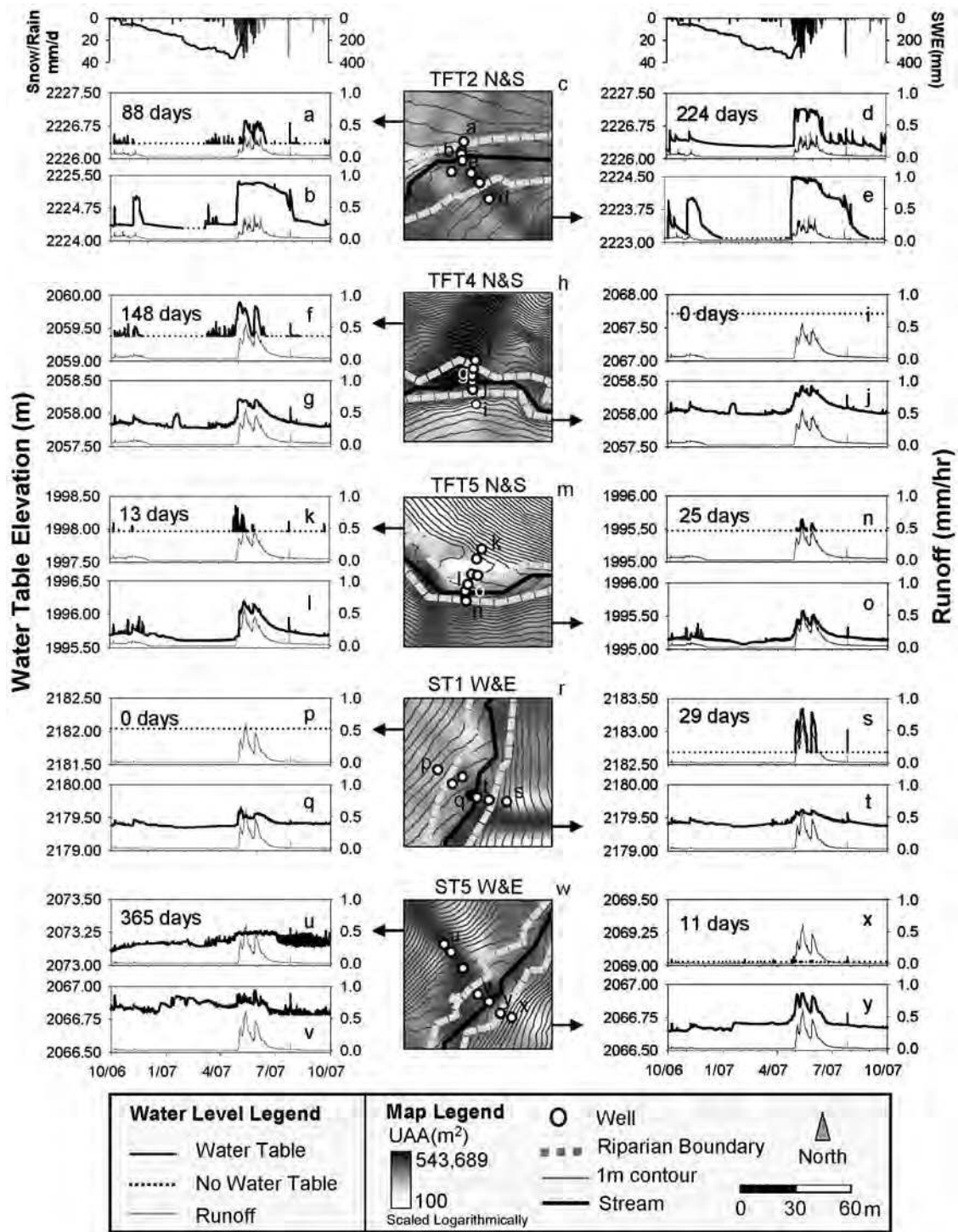
Figure 5. Transect hillslope and riparian water table and runoff dynamics. Runoff for each transect was obtained from the nearest flume location. The total time of HRS connectivity (days) is listed on the upper left corner of each hillslope time series. Maps are each transects UAA, riparian extents, and well locations. Letters on the map designate the location of hillslope and riparian well where water table dynamics were measured.

within a given catchment, to other catchments, or to development of general principles. We utilized an extensive well network across 24 HRS transects and catchment sizes from 0.4 to 23 km² to develop methods to scale plot-scale measurements of the hydrologic processes that link hillslopes and riparian areas to whole catchments and transfer our understanding to larger portions of the landscape. Our analyses included landscape level topographic analysis, process-based field investigations, and catchment-scale integration to identify the factors controlling the hydrologic connectivity between source areas generating runoff and the flow paths that link source areas to streams.
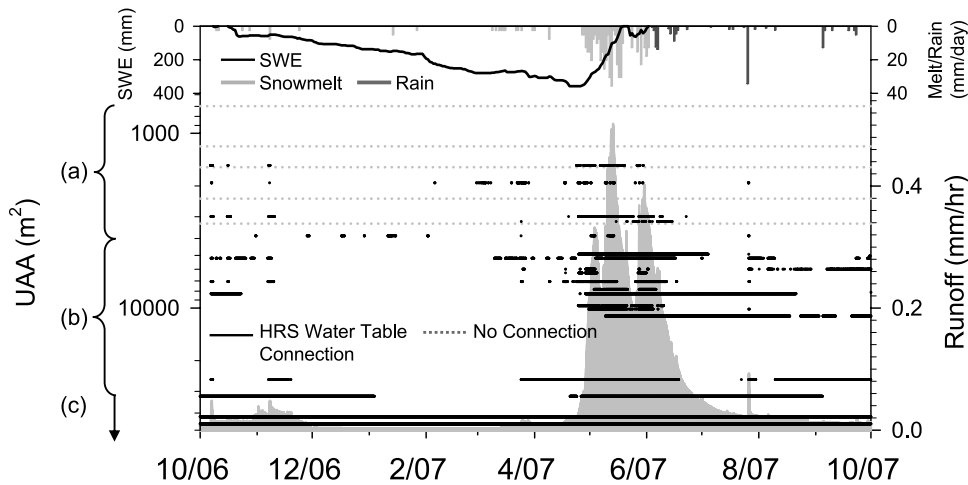
Figure 6. Binary summary of 24 transects of hillslope-riparian-stream water table connectivity dynamics for the 2007 water year. (a) Small UAA exhibits a transient connection or no connection. (b) Midrange UAA exhibits a sustained connection during large snowmelt and rain events and a transient connection during periods of low antecedent wetness. (c) Large UAA exhibits a continuous connection.

5.1. Does the Size of Hillslope UAA Explain the Development and Persistence of HRS Water Table Connectivity?

[40] Landscape assemblages exhibit different hydrologic thresholds depending on event size, antecedent moisture conditions, surface and bedrock topography [*Freer et al.*, 1997; *Sidle et al.*, 2000; *McGlynn et al.*, 2004] and distance from the stream [*Seibert et al.*, 2003]. This heterogeneity in space and time has previously hampered watershed-scale understanding. Once heterogeneity is integrated over sufficiently large spatial and temporal extents, however, emergent behavior may become apparent. Our high-frequency continuous observations of 24 transects of water level data indicated that the location, duration, and timing of hillslope water table development and its connectivity to the stream was controlled by the magnitude of UAA measured at each transects toe-slope well.

[41] The relationship between UAA and HRS hydrologic connectivity is evident in the duration of connectivity at each transect. Hillslope water levels never existed or were transient (Figure 6a) along transects with small UAAs. Figures 5k and 5x indicate that even during peak snowmelt, when soil wetness was at its annual maxima, only a brief water table response, on the order of hours to days, occurred along hillslope landscape elements with low UAA. The hillslope water table quickly subsided after this period of maximum wetness. We attribute transient connectivity in transects with small UAA to the limited accumulation of contributing area (and therefore water) along their downslope flow paths.

[42] Convergence of subsurface water into hillslope zones with medium to large UAA caused a sustained water table response at the base of hillslopes (Figures 5a, 5d, 5f, 5s, and 5u). Once HRS connectivity was established, lateral slope drainage, and periodic rejuvenation of hillslope soil moisture from events sustained the larger UAA hillslope water tables and the resulting HRS water table connection. In some cases the connection lasted from snowmelt well into the recessional period. The two transects possessing the

largest hillslope UAA inflows, ST2W and ST5W, remained hydrologically connected for the entire year (Figures 5u and Figure 6c).

[43] Water table initiation, cessation, and duration varied between transects partially as a function of UAA size, however variance was observed between transects with comparable UAA (Figure 6). The duration of HRS connectivity for 8 of the 24 transects under observation fall outside of the 95% confidence limits of equation (1). These timing differences may be attributed to the geometry (curvature, slope, etc.) of the UAA which can affect the "time of concentration" of snowmelt inputs. In addition, differences
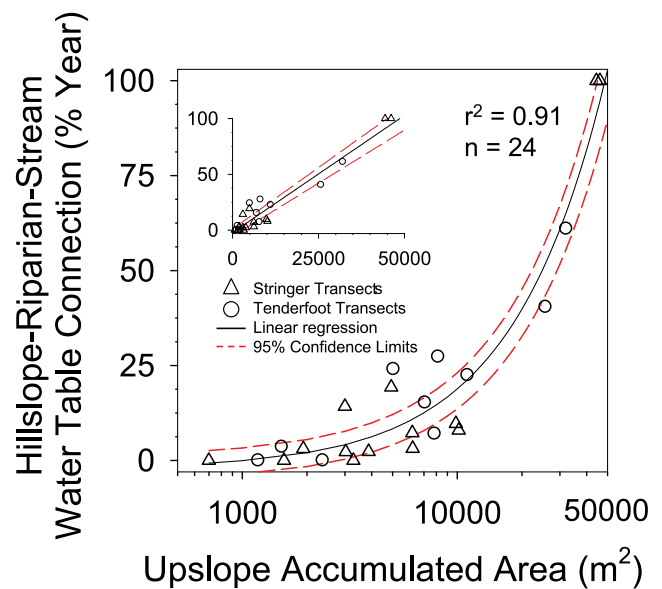
Figure 7. UAA regressed against the percentage of the water year that a hillslope-riparian-stream water table connection existed for 24 well transects. A connection was recorded when there was streamflow and water levels were recorded in both the riparian and hillslope wells. The inset plot shows the same data with a linear *x* axis.
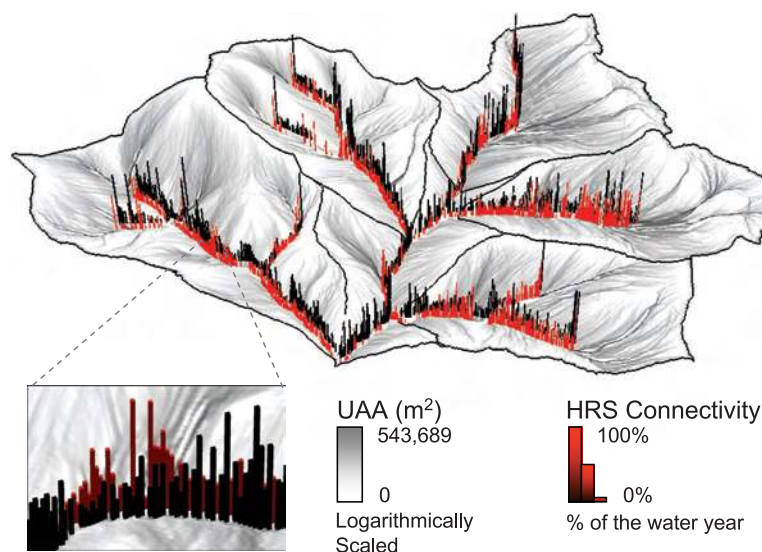
Figure 8. UAA flow accumulation patterns (shading) and the regression-derived hillslope-riparian-stream water table connectivity along the left (red bars) and right (black bars) sides of the Tenderfoot Creek network. Predicted hydrologic connectivity ranged from 0 to 100% of the year (represented by bar heights).

and combinations of aspect, precipitation/snowmelt variability, elevation, local soil and bedrock properties (including small differences in depth), vegetation, and antecedent wetness can all impact water table dynamics. Despite these differences, the overall response timing is coherent and suggests a strong UAA control on water table initiation, cessation, and duration across the TCEF catchment.

5.2. Can Topographic Analysis Be Implemented to Scale Observed Transect HRS Hydrologic Connections to the Stream Network and Catchment Scales?

[44] Analysis of our high-frequency measurements across 24 HRS assemblages indicated that the size of hillslope UAA controlled the development and persistence of HRS water table connectivity in TCEF. These results relating contrasting patterns of water table development to hillslope UAA size are consistent with past observations along individual landscape assemblages [*Dunne and Black*, 1970; *Harr*, 1977; *Anderson and Burt*, 1978] and hillslope trench sections [*Woods and Rowe*, 1996]. These prior observations were important for describing processes occurring at the plot scale, but they lacked a quantifiable framework, or relationship, for assessing the role of these source areas along the stream network and extrapolation to the catchment scale.

[45] When we regressed the duration of HRS connectivity for all 24 transects against their UAA size, the duration of landscape hydrologic connectedness was linearly related to the size of each transects UAA (Figure 7). This relationship provided a framework for estimating the duration of connectivity of each landscape source area along the stream network. We applied equation (1) to the UAA flowing into each stream pixel across Tenderfoot Creek (separated into each side of the stream). This distributed measure of landscape connectivity provided insight into the spatially and temporally variable hydrologic connectivity that existed for each landscape assemblage along the stream network throughout the year (Figure 8).

[46] Network connectivity results for TCEF indicated that runoff source area contributions were driven by transient connectivity during the wettest time periods. A high proportion of the Tenderfoot Creek network is composed of hillslopes with small UAA sizes (Figure 9a). Few of these hillslopes were hydrologically connected to their riparian and stream zones. For example, during the entire 2007 water year, a maximum of 67% of the stream network actually exhibited HRS water table connectivity (Figure 9b). The remaining 33% of the stream network, associated with the smallest UAAs remained disconnected for the entire year. As catchment wetness increased during snowmelt, small and medium UAAs developed hillslope water tables and became hydrologically connected. Landscape assemblages with small UAA accrued limited water year connectivity (0–8%), and then only after snowmelt and large rain events, in accordance with their transient hillslope responses. Only 10% of the stream network, associated with the medium to high ranged UAA inflows (Figure 9b), exceeded a 30% water year HRS water table connection. Approximately 2% of the TCEF stream network remained hydrologically connected for the entire water year (Figure 9b). These stream segments were associated with hillslopes possessing the largest UAA.

5.3. How Do Spatial Patterns and Frequency of Landscape Hydrologic Connectivity Relate to Catchment Runoff Dynamics?

[47] The relationship between UAA and the duration of hillslope-riparian-stream water table connectivity was linear (Figure 7). However, the distribution of UAA sizes along the network was heterogeneous and highly nonlinear due to catchment structure and topographic convergence and divergence in the landscape (Figure 9a). Since UAA size controlled landscape level connectivity, the distribution of HRS connectivity across the stream network was also heterogeneous and nonlinear.

[48] We compared Tenderfoot Creek's frequency distribution of HRS connectivity (i.e., connectivity duration
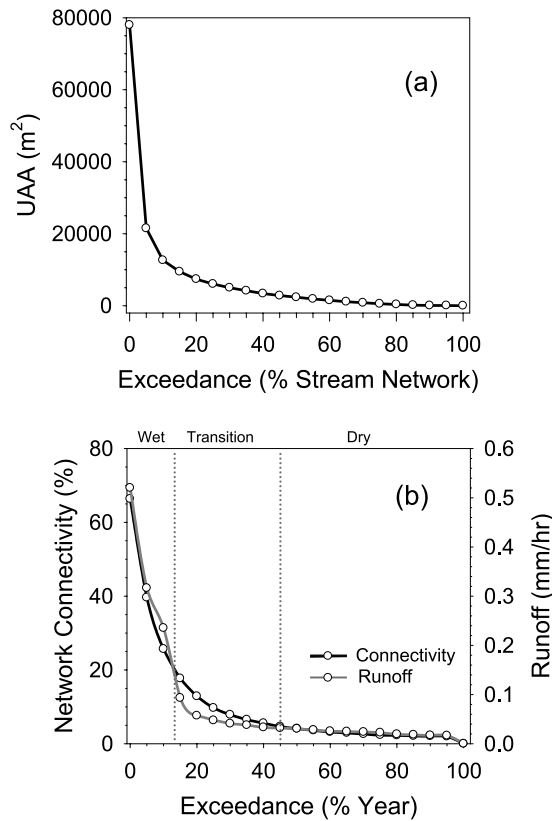
Figure 9. TCEF catchment. (a) UAA distribution curve based on 3108 10 m pixels along the stream network (both sides). (b) Comparison of the regression-derived connectivity duration curve (CDC) based on HRS water table connectivity for each 10 m UAA pixel along the stream network and the 2007 Lower Tenderfoot Creek flow duration curve (FDC). Periods of lowest runoff are associated with lowest network connectivity and large UAA values. Increased runoff is associated with increasing network connectivity from HRS connections at small UAA values.

curve, CDC) to its flow duration curve (FDC) to determine the relationship between network connectivity and the magnitude of catchment runoff through the year. The network CDC was strongly correlated ($r^2 = 0.95$) to the FDC (Figure 10a) over the full range of catchment wetness states. This suggests that the shape of the FDC is controlled by the fraction of the stream network hydrologically connected to its uplands throughout the year.

[49] To elucidate potential differences across catchment wetness states, we subdivided the annual relationship into dry, transition, and wet periods and found different relationships between the CDC and FDC for each period ($r^2 = 0.84$, 0.9 and 0.99, respectively.) This suggests that while the annual relationship was strong, there was different predictive power during each period, improving with increasing wetness.

[50] Dry fall and winter periods (55% of the year) corresponded to the lowest runoff (0.03 mm/h) and the lowest amount (<4%) of the stream network connected to its uplands (Figure 9b). The relationship between the CDC and FDC distributions during drier base flow periods ($r^2 = 0.84$, Figure 10b) indicates that HRS connectivity is one source of base flow runoff. However, three points of the distribution fall outside of the 95% confidence intervals during this time period. Consideration of other mechanisms such as bedrock flow paths [*Shaman et al.*, 2004; *Uchida et al.*, 2005] could help explain base flow runoff generation when the catchment is in a dry state.

[51] A break in slope (inflection point) of the stream FDC at ~0.05 mm/h corresponded to a paralleled increase in network connectivity (Figure 9b). These synchronous inflection points corresponded to early snowmelt and early summer dry-down which were the transition period between wet and dry catchment states. Greatest divergence in the FDC and CDC relationship was apparent during these transitions and may be related to the differential timing of water table connection-disconnection among areas with similar UAA sizes and riparian area saturation excess overland flow (Figures 9b and 10a). This divergence also corresponded to the region of the regression relationship (equation (1)) with the least robust model fit (Figure 7) Heterogeneity in slope, aspect, snowmelt timing, and soil
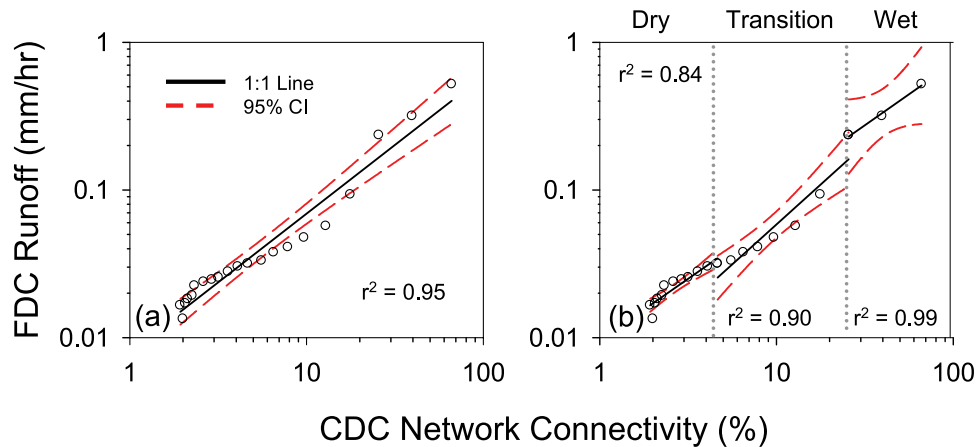
Figure 10. (a) Linear regression analysis between the estimated annual network CDC (3108 10 m pixels along both sides of the stream network) and the TCEF catchment FDC (8762 hourly measurements). (b) Linear regression for the same distributions separated into the dry, transitional, and wet catchment states. Each point represents 5% of the CDC and FDC distribution.

depth distributions would be most influential on the timing of HRS connectivity during transition periods and could explain some of the variability in the regression relationship. The correlation between the CDC and FDC (Figure 10b) improved (from $r^2 = 0.84$ to $r^2 = 0.90$) between the dry and transition periods. This improved correlation likely reflects increasing UAA/topographic controls on runoff production as the catchment became progressively wetter.

[52] During the wettest catchment states (snowmelt and the largest rain events), hillslopes associated with the smaller UAAs became hydrologically connected. The cumulative connections of small UAA coupled with previously connected medium and large UAAs, led to increasing network connectivity and subsequently larger magnitude runoff. During the highest flows (~10% of the year) up to 67% of the stream network was hydrologically connected to its uplands, resulting in peak runoff ranging from 0.24–0.54 mm/h (Figure 9b). The correlation between the CDC and FDC was also greatest during this time period ($r^2 = 0.99$). This suggests that the use of topographic metrics such as UAA as a surrogate for the lateral redistribution of water and prediction of runoff generation may be most robust during wetter time periods.

[53] Discretization of the annual relationship between the CDC and the FDC into dry, transition, and wet catchment states suggest that the relationship is strongest during wet periods. However, despite differential relationships for each wetness state, the annual relationship was robust ($r^2 = 0.95$) and suggests a single regression can explain most of the variability in the relationship between the CDC and FDC.

5.4. Implications

[54] Our observations highlight the importance of understanding hydrologic connectivity and how it is distributed in space and time along the stream network. The relationship between the FDC and CDC indicated that the period of time riparian and stream zones remain connected to their hillslope elements is highly related to catchment-scale runoff response (Figure 10a). Simply stated, the fraction of the network connected to its uplands controls runoff magnitude. These observations have important implications for modeling of catchment response to precipitation inputs and interpreting local process observations in the context of catchment runoff.

[55] Typically models of catchment response are developed from a sparse number of observations at a few points. It is assumed that the processes that occur in these locations are representative of other catchment locations and reflect dominant controls on catchment runoff. Runoff mechanisms including transmissivity feedback [*Kendall et al.*, 1999], piston flow displacement [*McGlynn and McDonnell*, 2003a], interflow [*Beven*, 1989], macropore flow [*McDonnell*, 1990], etc., are often used to explain threshold stream responses not predicted by limited process observations. These mechanisms do occur in many catchments [*McDonnell*, 1990b; *Buttle*, 1994; *Burns et al.*, 1998, 2001] and models incorporating them are often successful for mimicking individual hydrographs. However, difficulties arise when trying to predict stream response to multiple events across varying catchment wetness states, testing internal catchment consistency with model assumptions, and extrapolating to larger catchment sizes. These difficulties are partially a result of poor understanding of the spatial

sources of runoff through time across varying catchment wetness states.

[56] We suggest an alternate process explanation for nonlinear runoff response, namely the spatiotemporal distribution of connectivity. Our observations indicate that each landscape assemblage along the stream network exhibits a distinct time period of water table connectivity strongly related to its UAA. During driest times the largest UAA HRS assemblages are the primary contributors to stream runoff. As the amount of snowmelt or precipitation inputs increase more of the stream network associated with smaller UAA HRS assemblages becomes ''switched on'', and subsequently higher-magnitude runoff is generated. The magnitude of runoff is controlled by how many HRS assemblages along the stream network have reached their individual connectivity threshold, the duration of time they remain connected, and the amount of water flowing through them. These observed relationships suggest landscape structure (topography and topology) as a first-order control on runoff response characteristics.

[57] Given that at every point in time, a different fraction of the watershed is active in the runoff process (hydrologically connected via shallow groundwater to the stream channel); runoff biogeochemistry must also be interpreted in this context. We observed network connectivity ranging from ~4–67% of the stream network and suggest that biogeochemistry data interpretation and modeling should include appreciation of the dynamics of connectivity in space and time to attribute/represent appropriate causal mechanisms to runoff-biogeochemical observations. Hydrologic connectivity between catchment landscape elements is requisite for the retention or mobilization of dissolved organic carbon [*Boyer et al.*, 1997; *McGlynn and McDonnell*, 2003a], nutrients [*Creed et al.*, 1996; *Vidon and Hill*, 2004; *Ocampo et al.*, 2006] and other solutes[*Wilson et al.*, 1991; *Burns et al.*, 1998], to streams. For example, *Boyer et al.* [1997] demonstrated that the activation of shallow subsurface flow paths within the near stream saturated area was the dominant cause of DOC flushing in an alpine catchment. Implicit in this interpretation is lateral connectivity of the shallow groundwater flow paths that link the uplands and riparian areas to the stream network. The relationship between topographic metrics such as UAA and connectivity may provide a tool for identifying the location and duration of these lateral connections and testing their potential influence on stream water chemistry.

[58] The relationship between UAA and connectivity quantified in this study is likely nonstationary in time. The slope of the UAA:HRS water table connectivity relationship could increase or decrease between wet and dry years. However, the spatial pattern of connectivity is likely persistent due to the relatively static nature of landscape structure. This suggests that once a relationship is elucidated, fewer monitoring locations might be used to predict the slope of the UAA-connectivity duration relationship as a function of climatic variability. These results further suggest bidirectional prediction potential between the catchment flow duration curve and the catchment connectivity duration curve, providing a method for estimating network connectivity at a given runoff magnitude.

[59] This study is the first to identify relationships between catchment morphology and source area connectivity and

demonstrate how this integrated landscape-scale connectivity relates to the magnitude of catchment runoff. While the relationships between source area water table connectivity and whole catchment response have not previously been quantified, they are apparent in previous investigations relating the residence time of water to internal catchment structure [*McGlynn et al.*, 2003; *McGuire et al.*, 2005]. These studies found significant relationships for internal catchment topographic metrics including flow path length and gradient and median subcatchment area.

[60] Most studies seeking to link catchment topography to water redistribution have been conducted in headwater catchments sharing similar physical attributes: they tend to be located in steep mountainous landscapes; hillslope soils are shallow and underlain by relatively impervious bedrock; and valley-floor widths tend to be narrow relative to the width of the subtending catchment (i.e., Maimai, Hubbard Brook, Coweeta, HJ Andrews, etc.). The TCEF catchments compare favorably with these previous studies, suggesting that topographic control of whole catchment response may well be the norm in mountainous catchments.

[61] It remains an open question if topography or some other aspect of catchment structure will exert similarly strong control under other geomorphic and climatic conditions. For example, we could imagine that in areas with very low topographic relief, with deep soils and relatively shallow water tables, that precipitation inputs would percolate vertically through the soil profile until reaching the water table and the lateral redistribution of this water would then follow regional-scale groundwater flow paths. Under this scenario, groundwater inflows to stream would occur where ever stream channels intercept the regional water table so that runoff would not be strongly controlled by catchment topography. Conversely, even in areas of low topographic relief, during periods of high precipitation inputs (snowmelt season or large, long-duration rainstorms) some lateral redistribution of soil moisture occurs within the upper soil profile and would be affected by the topographic relations that we identify here. It is possible then, that some types of catchments might exhibit seasonal differences such that topography exerts primary control over catchment response during high flow but not during base flow [*Grayson et al.*, 1997; *Western et al.*, 1999]. Catchments underlain by highly fractured bedrock could also exhibit additional complexities and controls on water redistribution.

[62] More multiscale studies focused on landscape level hydrologic connectivity within a catchment-scale context, across a range of morphologic, climatic and topographic conditions, are needed to fully evaluate the relationships presented here. However, the relationships presented suggest that a measure of internal catchment topography and structure, easily measured from DEMs, may be used for a priori model development and prediction of hydrologic response. Measures of landscape element connectivity provide an integrated measure of hillslope process complexity and when integrated across the watershed provide a metric for prediction of runoff observed at the catchment outlet.

6. Conclusion

[63] How hillslope inputs along stream networks are linked to catchment-scale response has been poorly understood. Often, research is conducted along a specific plot/stream reach or at a single catchment scale. The results have therefore been plot and reach specific conclusions with little transferability to other catchments or development of general principles. We developed a metric of hillslope-riparian-stream water table connectivity as an integrative measure of runoff source area contributions through time. We tested this metric across 24 hillslope-riparian-stream landscape assemblages for the 2007 water year. On the basis of analysis of our high-frequency, long-duration observations coupled within a landscape analysis framework we conclude:

[64] 1. The topographically driven lateral redistribution of water (as represented by UAA) controls upland-stream connectivity and transient connectivity drives runoff generation through time.

[65] 2. This emerging space-time behavior represents the relationship between landscape structure/topology and runoff dynamics.

[66] 3. Analysis of catchment structure provides a context for scaling source area dynamics to those observed at the catchment outlet and provides a framework for exploring the spatially explicit links between source area connectivity and runoff generation.

[67] 4. Bidirectional prediction (as evidenced by the CDC-FDC relationship) of runoff generation and source area dynamics may be possible through analysis of catchment structure and topology.

[68] We have presented a landscape analysis framework for identifying runoff source areas based on their topographic characteristics (UAA). Where hydrologic connectivity occurs and the duration of these connections across the catchment is critical to guiding model development and understanding the link between landscape structure and stream flow. Future endeavors incorporating landscape analysis may include application of the terrain-morphology connectivity relationship across a range of catchments with different morphologies and antecedent conditions. These relationships may also prove valuable for linking internal landscape structure to stream nutrient and chemical signatures.

Appendix A: Detailed Description of HRS Water Table Response Dynamics

[69] We present detailed results for a subset of transects characteristic of the primary HRS landscape assemblages found within TCEF, their associated water table responses, and their hydrologic connectivity frequency and duration. These are: the headwaters of Upper Tenderfoot Creek (TFT2N and S), Middle Tenderfoot Creek (TFT4N and S), the outlet of Tenderfoot Creek (TFT5N and S), the headwaters of Stringer Creek (ST1E and W), and Middle Stringer Creek (ST5E and W).

A1. Tenderfoot Transect 2 North

[70] TFT2N groundwater table dynamics exhibited responses typical of headwater catchment landscape assemblages with midrange hillslope UAA (5044 m^2), minimal riparian area (3.8 m), and gentle ($\sim$4.8°) upland slopes (Figure 5c). Similar water table dynamics were

exhibited at TFT1N and TFT1S which have similar topographic and accumulated area characteristics (Table 1), 840 m upstream. Transient hillslope and riparian water tables responses were observed during the base flow period in response to early snowmelt events (Figures 5a and 5b). Hillslope water levels at TFT2N were sustained for 41 days during the snowmelt period (Figure 5a). Throughout the recession period transient hillslope responses were observed for large rain events. At the onset of the snowmelt period the riparian water table rose 98 cm to the ground surface over a 3 day period (Figure 5b). The development of a riparian water table coincided with the emergence of streamflow at this headwater transect (visual observation). A sharp decrease in riparian water levels beginning on 8/9/07 also corresponded with the cessation of streamflow and a decrease of the hillslope water table at the adjacent TFT2S transect. HRS water table connectivity was observed for 24% of the year (88 days).

A2. Tenderfoot Transect 2 South

[71] TFT2S was located along a broad convergent hillslope (UAA = 32,111 m^2) with low- angle hillslopes (~5.8°), and a 19.6 m wide riparian zone (Figure 5c). Stream and riparian water table dynamics were similar to those discussed for the TFT2N transect (Figure 5e). Hillslope water tables were observed for the entire water year (Figure 5d). During the base flow and recession periods hillslope water levels remained ~84 cm below the ground surface. Dynamic responses to individual rain events were observed during these time periods. At the onset of the snowmelt period water levels rose 85 cm to the ground surface. This rise coincided with the establishment of riparian water tables in both TFT2N and TFT2S and the initiation of streamflow (visual observation) at this transect. Following the rain period hillslope water levels declined to base flow levels. The timing of this decline was synchronous with a gradual decrease in riparian water levels and a decrease in runoff at the UTC flume 1500 m downstream. Though the hillslope well at this transect recorded water for the entire year, a HRS connection was only observed for 61% of the year (224 days).

A3. Tenderfoot Transect 4 North

[72] TFT4N was located along the main stem of Tenderfoot Creek near the base of a large convergent talus slope (UAA = 25,753 m^2) with ~22°hillslopes and a 9.3 m wide riparian zone (Figure 5h). Soil (60 cm on hillslopes, 80 cm in riparian zones) was only present on the lower portions of the hillslope where the monitoring wells were installed. The riparian water table remained ~40 cm below the ground surface during base flow and recession periods and rose to the ground surface during snowmelt (Figure 5g). Hillslope responses to snowmelt and rain events during both the base flow and recession periods were rapid and transient (Figure 5f). At the onset of snowmelt, the hillslope water table developed (rising 50 cm from base flow conditions) 7 days before increased runoff was observed at the Lower Tenderfoot flume. Hillslope water levels were recorded from the late base flow period, through snowmelt, to the end of the rain period. HRS connectivity was observed for 41% of the water year (147.6 days).

A4. Tenderfoot Transect 4 South

[73] TFT4S was selected as an end-member in the hillslope-riparian-stream continuum. Near the transects hillslope base, a ~42°, 10 m cliff effectively disconnected the small hillslope UAA (1,186) from its 4.4 m wide riparian zone below (Figure 5h). Riparian water level fluctuations mimicked those of streamflow measured at the LTC flume (Figure 5j) and the stream stage recorder located along this transect. No water was recorded in the hillslope well located near the precipice of the cliff approximately 10 m above the riparian zone (Figure 5i). Hillslope-riparian-stream water table connectivity was not observed at this transect location.

A5. Tenderfoot Transect 5 North

[74] TFT5N water table responses were typical of landscape positions with steep (~26°) divergent hillslopes, small UAA (1,527 m^2), and moderately wide (9.1 m) talus abundant riparian zones (Figure 5m). Riparian water table dynamics were similar to the stream hydrograph as recorded at the Lower Tenderfoot Creek flume and rose to within 15 cm of the ground surface during snowmelt (Figure 5l). The hillslope water table responses to rain and snow events were rapid and transient (Figure 5k). Small, ~12 cm rises were observed during the early base flow period. At the onset of the snowmelt period, water tables were observed in the hillslope well 2 days before rises in the riparian and stream water levels. During peak snowmelt, progressive diurnal water table increases and subsequent decreases of up to 40 cm were observed. HRS connectivity was observed for 4% of the water year (13.2 days).

A6. Tenderfoot Transect 5 South

[75] TFT5S groundwater table dynamics exhibited responses characteristic of headwater catchment landscape positions with moderate hillslope UAA (7,842 m^2), steep hillslopes (~37°), and small (2.9 m) riparian areas (Figure 5m). Riparian water table dynamics were synchronous with runoff, rising 40 cm up to the ground surface during snowmelt (Figure 5o). Hillslope water tables were observed only 10 days after substantial rises in the riparian water table during peak snowmelt and remained elevated for 26 days (Figure 5n). HRS connectivity was observed for 7% of the water year (25 days).

A7. Stringer Transect 1 West

[76] ST1W is situated along a planar hillslope, with diffuse inputs of UAA (Figure 5r). Water table responses were characteristic of landscape assemblages possessing low UAA (1563 m^2), moderate riparian zones (12.7 m), and upland slopes (~12.5°). The riparian water table remained within 20 cm of the ground surface for the majority of the water year, with near surface saturation during snowmelt and rain events (Figure 5q). The adjacent hillslope remained disconnected for the entirety of the

study period (Figure 5p). HRS water table connectivity was not observed at this transect.

A8. Stringer Transect 1 East

[77] Located near the base of a convergent hillslope hollow, ST1E (Figure 6r) groundwater dynamics exhibited responses typical of landscape positions with midrange UAA (10,165 m^2), moderate riparian widths (11.8 m), and moderate upland slopes (∼15.6°). Riparian zone water tables remained within 20 cm of the ground surface for the entire year with surface saturation during snowmelt and rain events (Figure 6t). A Hillslope water table was observed for the first time on 12 May 2006, exhibiting a rapid water table rise and sustained connection to its associated riparian zone (Figure 5s). These rapid water table rises and sustained HRS connections were observed during snowmelt (21 day connection) and the subsequent rain periods (8 day connection). A final connection was observed during the summer thunderstorm during the recession period. HRS water table connectivity was observed for 8% (29.2 days) of the water year at ST1E.

A9. Stringer Transect 5 West

[78] ST5W is located at the base of a convergent hillslope (Figure 5w). It had the largest observed UAA (46,112 m^2), a wide riparian zone (16.5 m) and ∼20.5° hillslopes. The riparian zone exhibited a relatively constant water table approximately 65 cm below the ground surface but rose to within 12 cm of the ground surface during the snowmelt and rain periods (Figure 5v). Groundwater was recorded within 15 cm of the ground surface in the hillslope well, located 5 m upslope of the toeslope break, for the duration of the water year (Figure 5u). Surface saturation and return flow (visual observations) at the toeslope transition occurred during snowmelt and large rain events. HRS water table connectivity was observed for the entire year at ST5W.

A10. Stringer Transect 5 East

[79] ST5E is located along a moderately steep (∼26°), divergent hillslope (UAA = 1923 m^2) with a 7.7 m wide riparian zone (Figure 5w). Riparian water levels remained between 80 and 60 cm below the ground surface throughout the year except during snowmelt when it rose to within 25 cm of the ground surface (Figure 5y). Hillslope water table responses to events were rapid and transient (Figure 5x). Water levels in the hillslope well were observed during the base flow period in response to minor snowmelt events. During peak snowmelt and the summer thunderstorm hillslope water tables of 2 to 10 cm were sustained for a maximum of two days. HRS connectivity was observed for 3% (11.2 days) of the water year.

References

Anderson, M. G., and T. P. Burt (1978), The role of topography in controlling throughflow generation, *Earth Surf. Processes Landforms*, 3, 331–334.

Beven, K. J. (1978), The hydrological response of headwater and sideslope areas, *Hydrol. Sci. Bull.*, 23, 419–437.

Beven, K. (1989), Interflow, in *Unsaturated Flow in Hydrologic Modeling Theory and Practice*, edited by H. J. Morel-Seyoux, pp. 191–219, Springer, New York.

Beven, K. J., and M. J. Kirkby (1979), A physically based, variable contributing area model of basin hydrology, *Hydrol. Sci. J.*, 24, 43–69.

Boyer, E. W., G. M. Hornberger, K. E. Bencala, and D. M. McKnight (1997), Response characteristics of DOC flushing in an alpine catchment, *Hydrol. Processes*, 11(12), 1635–1647, doi:10.1002/(SICI)1099-1085(19971015)11:12<1635::AID-HYP494>3.0.CO;2-H.

Burns, D. A., R. P. Hooper, J. J. McDonnell, J. E. Freer, C. Kendall, and K. Beven (1998), Base cation concentrations in subsurface flow from a forested hillslope: The role of flushing frequency, *Water Resour. Res.*, 34(12), 3535–3544, doi:10.1029/98WR02450.

Burns, D. A., J. J. McDonnell, R. P. Hooper, N. E. Peters, J. E. Freer, C. Kendall, and K. Beven (2001), Quantifying contributions to storm runoff through end-member mixing analysis and hydrologic measurements at the Panola Mountain Research Watershed (Georgia, USA), *Hydrol. Processes*, 15, 1903–1924, doi:10.1002/hyp.246.

Burt, T. P., L. S. Matchett, K. W. T. Goulding, C. P. Webster, and N. E. Haycock (1999), Denitrification in riparian buffer zones: The role of floodplain hydrology, *Hydrol. Processes*, 13(10), 1451–1463, doi:10.1002/(SICI)1099-1085(199907)13:10<1451::AID-HYP822>3.0.CO;2-W.

Buttle, J. M. (1994), Isotope hydrograph separations and rapid delivery of pre-event water from drainage basins, *Prog. Phys. Geogr.*, 18(1), 16–41, doi:10.1177/030913339401800102.

Buttle, J. M., S. W. Lister, and A. R. Hill (2001), Controls on runoff components on a forested slope and implications for N transport, *Hydrol. Processes*, 15, 1065–1070, doi:10.1002/hyp.450.

Buttle, J. M., P. J. Dillon, and G. R. Eerkes (2004), Hydrologic coupling of slopes, riparian zones and streams: An example from the Canadian Shield, *J. Hydrol.*, 287(1–4), 161–177, doi:10.1016/j.jhydrol.2003.09.022|ISSN 0022–1694.

Carlyle, G. C., and A. R. Hill (2001), Groundwater phosphate dynamics in a river riparian zone: Effects of hydrologic flowpaths, lithology, and redox chemistry, *J. Hydrol.*, 247, 151–168, doi:10.1016/S0022-1694(01)00375-4.

Covino, T. P., and B. L. McGlynn (2007), Stream gains and losses across a mountain-to-valley transition: Impacts on watershed hydrology and stream water chemistry, *Water Resour. Res.*, 43, W10431, doi:10.1029/2006WR005544.

Creed, I. F., L. E. Band, N. W. Foster, I. K. Morrison, J. A. Nicolson, R. S. Semkin, and D. S. Jeffries (1996), Regulation of nitrate-N release from temperate forests: A test of the N flushing hypothesis, *Water Resour. Res.*, 32(11), 3337–3354, doi:10.1029/96WR02399.

Devito, K. J., A. R. Hill, and N. Roulet (1996), Groundwater-surface water interactions in headwater forested wetlands of the Canadian Shield, *J. Hydrol.*, 181, 127–147, doi:10.1016/0022-1694(95)02912-5.

Dietrich, W. E., and T. Dunne (1993), The channel head, in *Channel Network Hydrology*, edited by K. Beven and M. Kirkby, pp. 175–220, John Wiley, Chichester, UK.

Dunne, T., and R. D. Black (1970), Partial area contributions to storm runoff in a small New England watershed, *Water Resour. Res.*, 6(5), 1296–1311, doi:10.1029/WR006i005p01296.

Farnes, P. E., R. C. Shearer, W. W. McCaughey, and K. J. Hanson (1995), Comparisons of hydrology, geology and physical characteristics between Tenderfoot Creek Experimental Forest (East Side) Montana, and Coram Experimental Forest (West Side) Montana, *Final Rep. RJVA-INT-92734*, 19 pp., For. Sci. Lab., USDA For. Serv. Intermountain Res. Stn., Bozeman, Mont.

Freer, J., J. McDonnell, K. J. Beven, D. Brammer, R. P. Hooper, and C. Kendall (1997), Topographic controls on subsurface storm flow at the hillslope scale for two hydrologically distinct small catchments, *Hydrol. Processes*, 11, 1347–1352, doi:10.1002/(SICI)1099-1085(199707)11:9<1347::AID-HYP592>3.0.CO;2-R.

Freeze, A. R. (1972), Role of subsurface flow in generating surface runoff: 2. Upstream source areas, *Water Resour. Res.*, *8*(5), 1272–1283, doi:10.1029/WR008i005p01272.

Grayson, R. B., A. W. Western, F. H. S. Chiew, and G. Bloschl (1997), Preferred states in spatial soil moisture patterns: Local and nonlocal controls, *Water Resour. Res.*, *33*(12), 2897–2908, doi:10.1029/97WR02174.

Harr, R. D. (1977), Water flux in soil and subsoil on a steep forested slope, *J. Hydrol.*, *33*, 37–58, doi:10.1016/0022-1694(77)90097-X.

Hewlett, J. D., and A. R. Hibbert (1967), Factors affecting the response of small watersheds to precipitation in humid areas, in *Forest Hydrology*, edited by W. E. Sopper and H. W. Lull, pp. 275–291, Pergamon, New York.

Hill, A. R. (2000), Stream chemistry and riparian zones, in *Streams and Ground Waters*, pp. 83–110, Academic, San Diego, Calif.

Holdorf, H. D. (1981), Soil resource inventory, Lewis and Clark National Forest: Interim in service report, Lewis and Clark Natl. For., For. Supervisor's Off, Great Falls, Mont.

Kendall, K. A., J. B. Shanley, and J. J. McDonnell (1999), A hydrometric and geochemical approach to test the transmissivity feedback hypothesis during snowmelt, *J. Hydrol.*, *219*(3–4), 188–205, doi:10.1016/S0022-1694(99)00059-1.

McDonnell, J. J. (1990), Rationale for old water discharge through macropores in a steep, humid catchment, *Water Resour. Res.*, *26*, 2821–2832.

McGlynn, B. L., and J. J. McDonnell (2003a), Role of discrete landscape units in controlling catchment dissolved organic carbon dynamics, *Water Resour. Res.*, *39*(4), 1090, doi:10.1029/2002WR001525.

McGlynn, B. L., and J. J. McDonnell (2003b), Quantifying the relative contributions of riparian and hillslope zones to catchment runoff, *Water Resour. Res.*, *39*(11), 1310, doi:10.1029/2003WR002091.

McGlynn, B. L., and J. Seibert (2003), Distributed assessment of contributing area and riparian buffering along stream networks, *Water Resour. Res.*, *39*(4), 1082, doi:10.1029/2002WR001521.

McGlynn, B. L., J. J. McDonnell, J. B. Shanley, and C. Kendall (1999), Riparian zone flowpath dynamics during snowmelt in a small headwater catchment, *J. Hydrol. Amsterdam*, *222*(1–4), 75–92, doi:10.1016/S0022-1694(99)00102-X.

McGlynn, B. L., J. J. McDonnell, and J. J. Bammer (2002), A review of the evolving perceptual model of hillslope flow paths at the Maimai catchments, *N. Z. J. Hydrol.*, *257*, 1–26.

McGlynn, B., J. McDonnell, M. Stewart, and J. Seibert (2003), On the relationships between catchment scale and streamwater mean residence time, *Hydrol. Processes*, *17*(1), 175–181, doi:10.1002/hyp.5085.

McGlynn, B. L., J. J. McDonnell, J. Seibert, and C. Kendall (2004), Scale effects on headwater catchment runoff timing, flow sources, and groundwater-streamflow relations, *Water Resour. Res.*, *40*, W07504, doi:10.1029/2003WR002494.

McGuire, K. J., J. J. McDonnell, M. Weiler, C. Kendall, B. L. McGlynn, J. M. Welker, and J. Seibert (2005), The role of topography on catchment-scale water residence time, *Water Resour. Res.*, *41*, W05002, doi:10.1029/2004WR003657.

Ocampo, C. J., M. Sivapalan, and C. Oldham (2006), Hydrological connectivity of upland-riparian zones in agricultural catchments: Implications for runoff generation and nitrate transport, *J. Hydrol.*, *331*(3–4), 643–658, doi:10.1016/j.jhydrol.2006.06.010.

Peters, D. L., J. M. Buttle, C. H. Taylor, and B. D. LaZerte (1995), Runoff production in a forested, shallow soil, Canadian Shield basin, *Water Resour. Res.*, *31*(5), 1291–1304, doi:10.1029/94WR03286.

Seibert, J., and B. L. McGlynn (2007), A new triangular multiple flow direction algorithm for computing upslope areas from gridded digital elevation models, *Water Resour. Res.*, *43*, W04501, doi:10.1029/2006WR005128.

Seibert, J., K. Bishop, A. Rodhe, and J. J. McDonnell (2003), Groundwater dynamics along a hillslope: A test of the steady state hypothesis, *Water Resour. Res.*, *39*(1), 1014, doi:10.1029/2002WR001404.

Shaman, J., M. Stieglitz, and D. Burns (2004), Are big basins just the sum of small catchments?, *Hydrol. Processes*, *18*(16), 3195–3206, doi:10.1002/hyp.5739.

Sidle, R. C., Y. Tsuboyama, S. Noguchi, I. Hosoda, M. Fujieda, and T. Shimizu (2000), Stormflow generation in steep forested headwaters: A linked hydrogeomorphic paradigm, *Hydrol. Processes*, *14*(3), 369–385, doi:10.1002/(SICI)1099-1085(20000228)14:3<369::AID-HYP943>3.0.CO;2-P.

Stieglitz, M., J. Shaman, J. McNamara, V. Engel, J. Shanley, and G. W. Kling (2003), An approach to understanding hydrologic connectivity on the hillslope and the implications for nutrient transport, *Global Biogeochem. Cycles*, *17*(4), 1105, doi:10.1029/2003GB002041.

Uchida, T., Y. Asano, Y. Onda, and S. Miyata (2005), Are headwaters just the sum of hillslopes?, *Hydrol. Processes*, *19*(16), 3251–3261, doi:10.1002/hyp.6004.

Vidon, P. G. F., and A. R. Hill (2004), Landscape controls on nitrate removal in stream riparian zones, *Water Resour. Res.*, *40*, W03201, doi:10.1029/2003WR002473.

Welsch, D. L., C. N. Kroll, J. J. McDonnell, and D. A. Burns (2001), Topographic controls on the chemistry of subsurface stormflow, *Hydrol. Processes*, *15*, 1925–1938, doi:10.1002/hyp.247.

Western, A. W., R. B. Grayson, G. Blöschl, G. R. Willgoose, and T. A. McMahon (1999), Observed spatial organization of soil moisture and its relation to terrain indices, *Water Resour. Res.*, *35*, 797–810, doi:10.1029/1998WR900065.

Wilson, G. V., P. M. Jardine, R. J. Luxmoore, L. W. Zelazny, D. A. Lietzke, and D. E. Todd (1991), Hydrogeochemical processes controlling subsurface transport from an upper subcatchment of Walker Branch watershed during storm events: 1. Hydrologic transport processes, *J. Hydrol.*, *123*, 297–316, doi:10.1016/0022-1694(91)90096-Z.

Woods, R. A., and L. K. Rowe (1996), The changing spatial variability of subsurface flow across a hillside, *N. Z. J. Hydrol.*, *35*, 51–86.

K. E. Bencala, U.S. Geological Survey, 345 Middlefield Road, Menlo Park, CA 94025, USA.

M. N. Gooseff, Department of Civil and Environmental Engineering, Pennsylvania State University, 212 Sackett Building, University Park, PA 16802, USA.

K. G. Jencso, L. A. Marshall, and B. L. McGlynn, Department of Land Resources and Environmental Sciences, Montana State University, Bozeman, MT 59717, USA. (kelsey.jencso@myportal.montana.edu)

S. M. Wondzell, Olympia Forestry Sciences Laboratory, Pacific Northwest Research Station, U.S. Forest Service, Olympia, WA 98512, USA.